Archives of Acoustics Vol. 51, No. 2, pp. 293–299 (2026), https://doi.org/10.24423/archacoust.2026.4396

Research Paper

The Mechanism of Formation of the Cutoff Frequency in an Acousto-Optic Delay Line and Some Proposals for its Measurement

Afig Hasanov, Ruslan Hasanov, Elgun Aghayev*, Rovshan Ahmadov

Department of Radio Electronics, National Aviation Academy
Baku, Azerbaijan

*Corresponding Author: eaghayev@naa.edu.az

Received December 14, 2025; revised February 23, 2026; accepted March 20, 2026; available online April 1, 2026; version of record June 3, 2026; published issue June 24, 2026.

The structure of the acousto-optic delay line and possible areas of its application are discussed. The necessity of determining the cutoff frequency of the acousto-optic delay line in all areas of its application is substantiated. The relationship between the cutoff frequency of an electric circuit and its time constant is discussed. The obtained result is extrapolated to the acousto-optic delay line, in which the cutoff frequency is formed by a completely different mechanism. The mechanism of cutoff frequency formation in the acousto-optic delay line is discussed. It is shown that the cutoff frequency in the acousto-optic delay line is formed due to the finite velocity of interaction of the acoustic wave with the light beam in the photoelastic medium. Two methods for measuring the cutoff frequency of the acousto-optic delay line are discussed: the method of system-parametric measurement and the method of cursor measurement. The system-parametric method for measuring the cutoff frequency of the acousto-optic delay line is implemented based on the known values of the laser beam diameter and the velocity of propagation of the acoustic wave in the photoelastic medium. The cursor method for measuring the cutoff frequency of the acousto-optic delay line is implemented based on the parameters of the oscillogram of its response to the input action in the form of a rectangular pulse. Theoretical and experimental aspects of the application of these methods are discussed. Corresponding numerical examples and experimental results are given.

Keywords: acousto-optic, delay line, cutoff frequency, transient response, system-parametric measurement, Bragg diffraction.

Copyright © 2026 The Author(s).
This work is licensed under the Creative Commons Attribution 4.0 International CC BY 4.0 (https://creativecommons.org/licenses/by/4.0/).

1. Introduction

An acousto-optic delay line (AODL) is implemented based on the photoelastic effect and is used to process signals in the time domain. AODL differs from other types of acousto-optic processors in that information it contains is extracted by a light beam whose diameter is significantly smaller than the size of the optical aperture of the interaction medium. In devices of this class, efficient signal processing in the time domain is due to the low velocity of propagation of the acoustic wave in the photoelastic medium (PEM), the ability to regulate the delay time of the electrical signal by simple mechanical movement of the interaction medium, and the ability to synthesize PEMs of sufficiently large sizes. The AODL can be used in radio engineering systems for various purposes, in radar target simulators (Diewald *et al.*, 2018; Okoń-Fąfara *et al.*, 2019), and also for solving other radar problems associated with the formation of time intervals (da Silva *et al.*, 2024; Daggula, Bevara, 2024; Russell *et al.*, 2025; Wu, 2025). Diewald *et al.* (2018) described a system capable of simulating the behavior of radar targets. Okoń-Fąfara *et al.* (2019) discussed the development of a radar air situation map simulator that can be used to train military radar operators, to evaluate the functionality of new radar

systems and signal processing algorithms without the need for physical equipment, etc. In both cases, digital devices capable of generating and processing signals with a limited spectrum are used. However, generating and processing broadband signals is very difficult or impossible.

The use of AODL in solving the problems considered in the indicated works allows for a significant expansion of the technical capabilities of the corresponding devices and systems. In all cases of application of the AODL, one of the main parameters is its cutoff frequency. The cutoff frequency of an arbitrary electrical circuit is defined as the frequency at which the output signal power is reduced by half from the original value. This parameter is determined by the structure of the electrical circuit and the reactive parameters of each node in its composition. Any electric circuit responds to an input action not instantly, but with a certain delay. This delay is usually estimated by the time constant of the transient response of the electric circuit. The time constant of the transient response of the electric circuit τ is defined as the time interval from the beginning of the formation of the output response to the input action in the form of a single-step to the moment when the value of this response reaches the level of $(1-1/e)\cdot 100 = 63.2\,\%$ of the steady-state value. The cutoff frequency of the electric circuit f_c is determined by the known value of its time constant τ as follows:

$$f_c = 1/(2\pi\tau). \tag{1}$$

From Eq. (1) it follows that, using any method that allows one to determine the time constant of an electric circuit, one can calculate its cutoff frequency. For example, in the case of an RC circuit, the time constant is defined as the product of the nominal values of the elements R and C. Accordingly, the formula for calculating the cutoff frequency (Eq. (1)) takes the following form: $f_c = 1/2\pi RC$. A similar statement is true for all electric (including radio engineering) circuits whose equivalent circuits can be represented as an RC circuit.

The cutoff frequency is also formed in the AODL, despite the obvious absence of reactive elements in its structure. The article is devoted to the structural interpretation of the mechanism for forming the cutoff frequency of an acousto-optic delay line and solving the problem of its measurement.

2. Material and method

In the AODL, the processed analog signal $u_{\text{in}}(t)$ is fed to the first input of the amplitude modulator (AM) (Fig. 1). The carrier oscillation from the high-frequency generator (HFG) is fed to the second input of the AM. An amplitude-modulated radio-frequency signal is formed at the AM output. It should be noted that, depending on the nature of the problem being solved, balanced amplitude modulation, frequency modulation, or amplitude manipulation can also be used. The amplitude-modulated signal at the AM output is described by the expression:

$$u_{\text{AM}}(t) = U_0[1 + m\cdot s(t)]\cdot\cos(\omega_0 t),$$

where U_0 is the amplitude, ω_0 is the carrier oscillation frequency, $s(t)$ is the modulating process, which changes within the limits $s(t) = \pm 1$. In our case $s(t) = u_{\text{in}}(t)/[u_{\text{in}}(t)]_{\max}$, where $[u_{\text{in}}(t)]_{\max}$ is the maximum value of the processed analog signal $u_{\text{in}}(t)$.

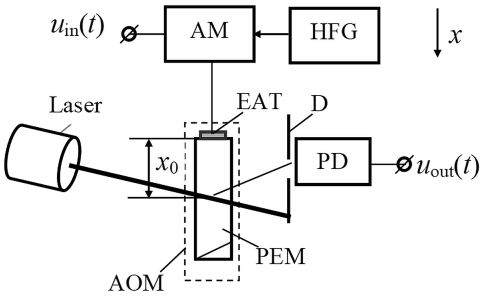

Fig. 1. Schematic diagram of an acousto-optic delay line.

The amplitude-modulated signal is transmitted to an electro-acoustic transducer (EAT) attached to the end of the PEM. The EAT excites an acoustic wave in the PEM, which propagates with a velocity v that is ~10^5 times smaller than the propagation velocity of an electromagnetic wave. A cell consisting of the PEM and the EAT attached to its end is called an acousto-optic modulator (AOM) (Davis, 2014; Molchanov *et al.* 2015). In this case, the frequency of the carrier oscillation ω_0 generated in the HFG is selected in the range of operating frequencies of the AOM, which, as a rule, is 40 % to 60 % of its central frequency (Yushkov *et al.*, 2024). The central frequency of the AOM can be selected from tens of MHz to units of GHz. It follows that when constructing an AODL, the value of the carrier oscillation frequency does not impose any special restrictions on its operational and technical characteristics, and it is possible to use existing ready-made units, in particular, the AOM. In this case, AM and HFG are used only to transfer the spectrum of the processed analog signal to the operating frequency range of the AOM.

The requirement for the maximum frequency of the modulating process $s(t)$ is formed based on the known value of the AODL cutoff frequency. The AODL cutoff frequency must be equal to or greater than the maximum frequency of the processed analog signal $u_{\text{in}}(t)$. In other words, the design and technological characteristics of the AODL must be adapted to the maximum frequency of the processed analog signal $u_{\text{in}}(t)$.

The circuit in Fig. 1 uses the Bragg diffraction mode. A laser beam of diameter d passing through the AOM is modulated by diffraction on inhomogeneities in permittivity caused by deformations of the PEM material under the action of an acoustic wave. Part of the light beam is deflected into the diffraction order. The deflected light falls through the hole in the diaphragm (D) onto the surface of the photodetector (PD) and is detected. As a result, a voltage $u_{\text{out}}(t)$ is formed at the PD output, which repeats the shape of the processed input signal $u_{\text{in}}(t)$ and lags behind it in time:

$$t_d = x_0/v, \tag{2}$$

where x_0 is the distance from the EAT to the acousto-optic interaction point in the PEM.

In other words, ideally for AODL the equality:

$$u_{\text{out}}(t) = c \cdot u_{\text{in}}(t - t_d), \tag{3}$$

holds, where c is a constant factor.

In a real AODL, equality (Eq. (3)) is fulfilled with distortions acceptable for practice in the frequency band limited by the cutoff frequency. This parameter is formed due to the finite speed of physical processes in the nodes that participate in the formation of the response at the AODL output. Abstracting from secondary factors, it can be assumed without proof that in the chain of nodes participating in the formation of the AODL cutoff frequency, the AOM and PD have an incomparably greater influence. When using a high-speed photomultiplier, for example a photomultiplier based on the FEU-114 type, its influence on the cutoff frequency of the AODL can also be neglected. Therefore, based on this interpretation of the operation of an AODL, it can be assumed that, under certain conditions, its cutoff frequency is formed by the final speed of intersection of a light beam with an acoustic wave in a photoelastic medium (Muromets *et al.*, 2016; Hasanov *et al.*, 2022). With these interacting wave parameters (the diameter of the light beam d and the velocity of propagation of the acoustic wave in the photoelastic medium v), the following expression can be obtained for the transient response of the AODL (Hasanov *et al.*, 2019):

$$g(t) = \frac{8}{\pi\left(\frac{d}{v}\right)^2} \cdot \int_{t_d}^{t} \sqrt{\frac{d}{v}(\xi - t_d) - (\xi - t_d)^2}\, \mathrm{d}\xi, \qquad \text{for} \quad t_d \le t \le t_d + \frac{d}{v}. \tag{4}$$

Equation (4) provides a concrete mathematical description of how an AODL responds to a single-step input signal, and allows us to predict and calculate the response of an AODL to virtually any conceivable input signal using the Duhamel integral. This makes Eq. (4) and the Duhamel integral a powerful combination for analyzing and predicting the behavior of an AODL under various operating conditions.

The graph of the transient response of the AODL, constructed using Eq. (4), with the parameter values $t_d = 0.1$ μs, $v = 3.63$ km/s, $d = 2.2$ mm is shown in Fig. 2.

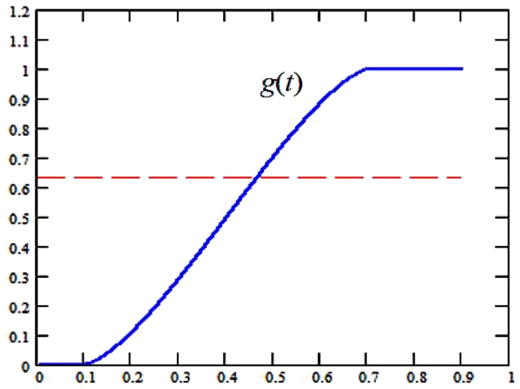

FIG. 2. Graph of the transient response of the AODL.

The time constant of the AODL (and, accordingly, its cutoff frequency) can be calculated both by the formula of the transient response (Eq. (4)) and by its graph (Fig. 2), which is the basis of two methods for measuring the cutoff frequency of the AODL. These methods are discussed further.

3. System-parametric method for measuring the cutoff frequency of an AODL

The system-parametric method for measuring the AODL cutoff frequency consists of determining the AODL time constant by its transient response based on known values of the parameters of the interacting beams (acoustic and optical). Then, the AODL cutoff frequency is calculated based on the known value of the time constant. From Eq. (4), the time constant of the AODL is determined as follows:

$$\tau = t_1 - t_d, \tag{5}$$

where $t_1 = t_d + \tau$ is the moment in time when the right side of Eq. (4) is equal to 0.632, i.e., the equality $g(t_1) = 0.632$ is satisfied.

The cutoff frequency f_c of a specific type of AODL does not depend on the value of the delay time t_d, which is determined by Eq. (2). From a joint analysis of Eq. (1) to Eq. (5), it is easy to conclude that, using known values of the parameters v and d, it is possible to calculate the cutoff frequency of the AODL with sufficient accuracy for engineering calculations. Calculations are easily performed in the Mathcad environment. Calculations are performed for the following values of the design parameters: $t_d = 0.1\,\mu s$, $v = 3.63\,km/s$, $d = 2.2\,mm$. Equating the right side of Eq. (4) to 0.632, we find the time constant of the AODL τ. Thus, for the time constant of the AODL we obtain the following value: $\tau = 0.366\,\mu s$. Accordingly, the cutoff frequency of the AODL, calculated using Eq. (1), is

$$f_c = 1/(2\pi \cdot 0.366) = 0.435\,MHz.$$

4. Cursor method for measuring the cutoff frequency of an AODL

The method of cursor measurement of the AODL cutoff frequency consists of determining its time constant based on the parameters of the oscillogram of its response to the pulse input signal. Then, based on the known value of the time constant, the AODL cutoff frequency is calculated.

In the experimental research model, a rectangular pulse with the required parameters is formed in the G5-54 pulse generator. The pulse from the G5-54 generator output modulates the oscillations of the G4-107 high-frequency generator (operates in the external pulse modulation mode) and synchronizes the MSO4052 oscilloscope. The oscillation frequency of the G4-107 generator is selected equal to the central frequency of the AOM, which in our experiments is 80 Hz. The deflected light in the rear focal plane of the AOM is recorded

by a PD based on a FEU-114 photoelectron multiplier. The devices in the laboratory setup are connected to each other by radio frequency cables.

The oscillograms of the voltages at the input and output of the AODL with the parameters t_d = 0.1 μs, v = 3.63 km/s, d = 2.2 mm, $\tau_i \approx 1.5$ μs are shown in Fig. 3.

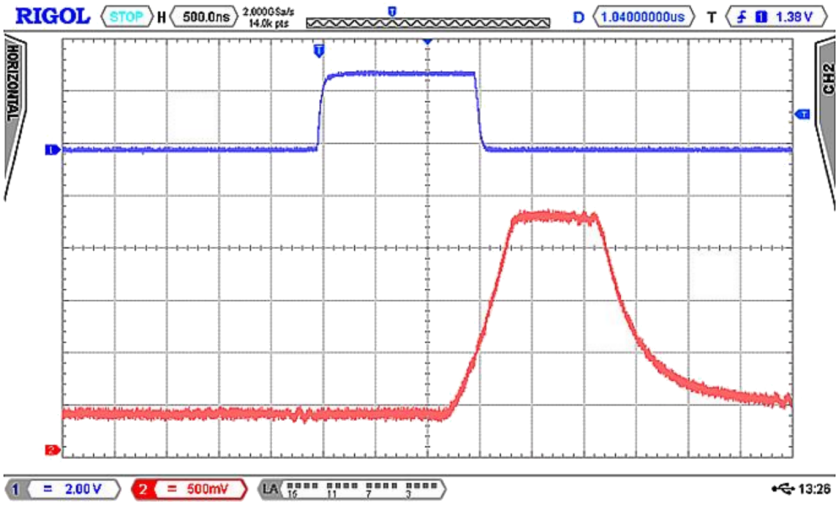

Fig. 3. Oscillograms of pulses at the input (1) and output (2) of an acousto-optic delay line.

The duration of the input pulse (determined from the oscillogram at a level of 0.5 of the maximum value) is equal to $\tau_i \approx 1.5$ μs. The time constant of the transient response, i.e., the time during which the response – the output voltage changes from 0 % to 63.2 % of its maximum value (≈1.9 V), is equal to approximately 380 ns, which coincides with the calculated values of the time constant of the transient response. The experimentally measured value of the AODL cutoff frequency is $1/(2\pi \cdot 0.38)$ = 419 kHz. Thus, the spread from the average value in the obtained results of system-parametric (435 kHz) and cursor (419 kHz) measurements does not exceed 5 %.

The discrepancy between the results of system-parametric and cursor measurements is primarily due to the influence of the photodetector. In the case of system-parametric measurements, the influence of the photodetector is not taken into account. However, the photodetector does contribute to the results of cursor measurements.

5. Results and discussion

When constructing an AODL for processing an analog signal, it is important to optimize the cutoff frequency in the context of the maximum signal frequency. The problem can be solved directly or indirectly. Direct measurement of the AODL cutoff frequency can be performed using an experimentally measured amplitude-frequency characteristic. To measure the amplitude-frequency characteristic, appropriate devices are needed. In addition, this takes a lot of time, especially if several measurements are required. Therefore, indirect measurement is more preferable. Indirect measurement of the cutoff frequency is possible using the system-parametric and cursor methods. The system-parametric method for measuring the AODL cutoff frequency appeals to a priori known values of the laser beam diameter and the acoustic wave propagation velocity in the PEM. The cursor method of measuring the AODL cutoff frequency is implemented by the parameters of its response to the input action in the form of a rectangular pulse. Accordingly, these methods can be used at various stages of the AODL development. At the design stage, it is preferable to use the system-parametric measurement, at the testing stage – the cursor measurement. From the interpretation of the measurements, it follows that the results obtained by different methods differ by no more than four percent. These errors are mainly due to the fact that the measurements were made using an oscillogram. With direct measurements, the accuracy will be much higher, since the digital oscilloscope provides measurements of time parameters with an accuracy of up to 0.0001 %.

In the presented methods for measuring the AODL cutoff frequency, the influence of the photodetector is not discussed. This is due to the fact that a high-speed photodetector is assumed to be used a priori. In this

case, a photodetector of the FEU-114 type was used, for which the rise time of the transient response, according to the passport data, is ≤9 ns. Subtracting this value from the cursor measurement result (380 ns) yields 371 ns. The corresponding AODL cutoff frequency is $1/(2\pi \cdot 0.371) = 429$ kHz, which is slightly different from the system-parametric measurement result (435 kHz). All this confirms the postulate that the AODL cutoff frequency is determined by the interaction time of the light and elastic wave.

6. Conclusion

One of the main parameters of the AODL is its cutoff frequency. This parameter is taken into account at the design stage, during operation and when analyzing the output results. The methods of system-parametric measurement and cursor measurement of the AODL cutoff frequency allow solving this problem quite simply and correctly. Based on these methods, it is possible to select the type of PEM material and the parameters of the light source (laser). The method of system-parametric measurement is used at the design stage. At the same time, this method can also be used to test the results of experimental studies.

Fundings

This research did not receive any specific grant from funding agencies in the public, commercial, or not-for-profit sectors.

Conflict of interest

The authors declare that they have no known competing financial interests or personal relationships that could have appeared to influence the work reported in this paper.

Authors' contributions

Afig Hasanov developed the method, prepared figures, and wrote the manuscript. Ruslan Hasanov, Elgun Aghayev, Rovshan Ahmadov conducted measurements and provided technical approval. All authors reviewed and approved the final manuscript.

References

1. da Silva R.E., Manuylovich E., Sahoo N., Franco M.A.R., Bartelt H., Webb D.J. (2024), All-fiber fast acousto-optic temporal control of tunable optical pulses, *Optical Fiber Technology*, **87**: 103877, https://doi.org/10.1016/j.yofte.2024.103877.
2. Daggula R., Bevara V. (2024), An ultra-low power QCA based vedic multiplier for digital radar application, *e-Prime – Advances in Electrical Engineering, Electronics and Energy*, **9**: 100695, https://doi.org/10.1016/j.prime.2024.100695.
3. Davis C.C. (2014), *Lasers and Electro-Optics*, Cambridge University Press.
4. Diewald A.R., Steins M., Müller S. (2018), Radar target simulator with complex-valued delay line modeling based on standard radar components, *Advances in Radio Science*, **16**: 203–213, https://doi.org/10.5194/ars-16-203-2018.
5. Hasanov A. *et al.* (2022), Development of an axonometric model of photoelastic interaction in an acousto-optic delay line and its approbation, *Technology Audit and Production Reserves*, **5**(2(67)): 38–45, https://doi.org/10.15587/2706-5448.2022.267782.
6. Hasanov A.R., Hasanov R.A., Ahmadov R.A., Agayev E.A. (2019), Time- and frequency-domain characteristics of direct-detection acousto-optic delay lines, *Measurement Techniques*, **62**: 817–824, https://doi.org/10.1007/s11018-019-01700-3.
7. Molchanov V.Ya. *et al.* (2015), *Theory and Practice of Modern Acousto-Optics* [in Russian], Publishing House MISiS.

8. Muromets A.V., Voloshinov V.B., Kononin I.A. (2016), Transmission characteristics of acousto-optic filter using sectioned transducer, *Applied Acoustics*, **112**: 221–225, https://doi.org/10.1016/j.apacoust.2016.04.008.

9. Okoń-Fąfara M., Kawalec A.M., Witczak A. (2019), Radar air picture simulator for military radars, [in:] *XII Conference on Reconnaissance and Electronic Warfare Systems*, **1105519**, https://doi.org/10.1117/12.2525032.

10. Russell R.S., Anderson B.E., Denison M.H. (2025), Using time reversal with long duration broadband noise signals to achieve high amplitude and a desired spectrum at a target location, *Applied Acoustics*, **236**: 110744, https://doi.org/10.1016/j.apacoust.2025.110744.

11. Wu M., Ma J., Zhang Q. (2025), Photonic-assisted angle-of-arrival measurement system for both broadband and single-frequency radar signals, *Optics Communications*, **577**: 131392, https://doi.org/10.1016/j.optcom.2024.131392.

12. Yushkov K.B., Naumenko N.F., Molchanov V.Ya. (2024), Design of a broadband acousto-optic filter using bulk acoustic wave beam steering with an interdigital transducer, *Results in Physics*, **59**: 107575, https://doi.org/10.1016/j.rinp.2024.107575.